

## **Wave Damping in Rubble Mounds**

Markus Muttray, Delta Marine Consultants b.v., Gouda, The Netherlands, m.muttray@dmc.nl  
Hocine Oumeraci, Leichtweiss Institute, Technical University Braunschweig, Germany,  
h.oumeraci@tu-bs.de  
Bas Reedijk, Delta Marine Consultants b.v., Gouda, The Netherlands, j.reedijk@dmc.nl

### **ABSTRACT**

*The wave damping in a rubble mound breakwater has been studied theoretically and experimentally. Various types of damping functions (linear, quadratic and polynomial) have been derived and checked against experimental results from large scale model tests. Damping coefficients have been derived from the hydraulic resistance of the breakwater core material. The result is a general approach for the wave decay inside a rubble mound breakwater that clearly reflects the flow processes inside the structure.*

### **INTRODUCTION**

While the main part of the incoming wave energy is reflected at the seaward face of a rubble mound breakwaters or dissipated at and inside the structure, some wave energy will pass through the breakwater and will cause wave disturbance at the lee side. The wave damping inside a breakwater and the wave transmission are a result of the turbulent, instationary and non-uniform porous flow inside the breakwater and thus difficult to quantify. Two-phase flow (air-water mixture) is further likely to occur in the seaward part of the structure.

In this paper a relatively simple analytical method is presented for the assessment of wave height attenuation inside a rubble mound breakwater. The method has been derived theoretically and validated against experimental results from large scale model tests. The new method reflects the actual physical processes inside the breakwater more than existing approaches and proved to be more accurate.

### **PREVIOUS WORK**

The hydraulic resistance  $I$  for instationary flow in coarse porous media can be approximated by the extended Forchheimer equation with an additional inertia term (POLUBARINOVA-KOCHINA, 1962):

$$I = a v_f + b v_f^2 + c \frac{\delta v_f}{\delta t} \quad \text{Eq. 1}$$

where  $a$ ,  $b$  and  $c$  are dimensional coefficients and  $v_f$  is the flow velocity inside the porous medium (filter velocity). A set of equations and coefficients to determine the hydraulic resistance of a rigid homogeneous, isotropic porous medium for single phase flow is summarised in Table 1 and Table 2 (for further details see MUTTRAY, 2000).

Linear resistance coefficient for stationary flow (KOZENY, 1927 and CARMAN, 1937)		$a = K_a \frac{(1-n)^2}{n^3} \frac{\mu}{gd^2}$	Eq. 2
with:	$n$ porosity $d$ grain size $K_a$ non-dimensional coefficient (see Table 2) $\mu$ kinematic viscosity		
Quadratic resistance coefficient for stationary flow (ERGUN, 1949)		$b = K_b \frac{1-n}{n^3} \frac{1}{gd}$	Eq. 3
with:	$K_b$ non-dimensional coefficient (see Table 2)		
Quadratic resistance coefficient for oscillatory flow (VAN GENT, 1993)		$b_{oscillating} = b_{stationary} \left( 1 + \frac{7.5}{KC} \right)$	Eq. 4
with:	$KC$ Keulegan-Carpenter number ( $KC = V_f T / (n d)$ )		
	$V_f$ velocity amplitude		
	$T$ period of the oscillatory porous flow		
Inertia coefficient (SOLLIT & CROSS, 1972)		$c = \frac{1}{n g} \left( 1 + K_M \frac{1-n}{n} \right)$	Eq. 5
Added mass coefficient (VAN GENT, 1993)		$K_M = \max \left\{ 0.85 - 0.015 \frac{n g T}{V_f} ; 0 \right\}$	

Table 1: Forchheimer resistance coefficients  $a$ ,  $b$  and  $c$  for stationary and oscillatory flow

Author	Characteristic particle diameter	Coefficients	
		$K_a$	$K_b$
Kozeny (1927); Carman (1937)	$d_{eq}$	180	–
Ergun (1949, 1952)	$d_{n50}$	150	1.75
Engelund (1953)	$d_{eq}$	–	1.8 – 3.6
Koenders (1985)	$d_{n15}$	250 – 330	–
den Adel (1987)	$d_{n15}$	75 – 350	–
Shih (1990)	$d_{n15}$	> 1684	1.72 – 3.29
Van Gent (1993)	$d_{n50}$	1000	1.1
The equivalent diameter $d_{eq}$ is the diameter of a sphere with mass $m_{50}$ and specific density $\rho_s$ of an average actual particle: $d_{eq} = (6 m_{50} / \pi \rho_s)^{1/3}$			
The nominal diameter $d_{n50}$ is the diameter of a cube with mass $m_{50}$ and specific density $\rho_s$ of an average actual particle: $d_{n50} = (m_{50} / \rho_s)^{1/3}$			

Table 2: Empirical coefficients and characteristic particle diameters for the Forchheimer coefficients  $a$  and  $b$  (stationary flow)

The wave propagation in a rubble mound breakwater has been investigated by HALL (1991, 1994) in small scale experiments and by BUERGER ET AL. (1988), OUMERACI & PARTENSKY (1990) und MUTTRAY ET AL. (1992, 1995) in large scale experiments. Field measurements have been conducted at the breakwater at Zeebrugge (TROCH ET AL. 1996, 1998).

The amplitude of the pore pressure oscillations inside the core increases with increasing wave height and wave period (OUMERACI & PARTENSKY, 1990) while the rise time of the pressure

oscillations remains almost constant (HALL, 1994). The pore pressure oscillations decrease in the direction of wave propagation. The damping of pore pressure oscillations increases with increasing wave height and decreases with increasing wave period (BUERGER ET AL., 1988; TROCH ET AL., 1996). The following approach has been proposed by OUMERACI & PARTENSKY (1990) for the variation of pore pressure oscillations in horizontal direction:

$$P(x) = P_0 \exp\left[-K_d \frac{2\pi}{L'} x\right] \quad \text{Eq. 6}$$

with dimensionless damping coefficient  $K_d$ , amplitude of pore pressure oscillations  $P_0$  (at position  $x = 0$ ) and  $P(x)$  (at varying position  $x > 0$ ) and wave length  $L'$  inside the structure. The exponential decrease has been confirmed in field measurements (TROCH ET AL., 1996).

### METHODOLOGY

The wave height attenuation inside a rubble mound breakwater has been analysed theoretically. A simple universal concept for the wave height decay inside the structure is derived by means of some simplifying assumptions. The theoretical results have been validated experimentally. Large scale model tests have been performed with a rubble mound breakwater with a typical cross section in order to prevent scale effects and to ensure that the results are properly transferred to prototype conditions. Furthermore, the experimental results were required to quantify non-linear effects that had been neglected in the theoretical approach and to approximate them by empirical means. The objective is a simple and relatively accurate description of wave damping inside a rubble mound breakwater, which clearly reflects the governing physical processes.

The analysis of the wave motion inside the breakwater is restricted to that part of the core, where the water surface remains inside the core during the entire wave cycle. Thus, only the breakwater core landward of the point of maximum wave run-up on the core is considered (see Figure 1) as further seaward the wave motion is affected by the breakwater slope.

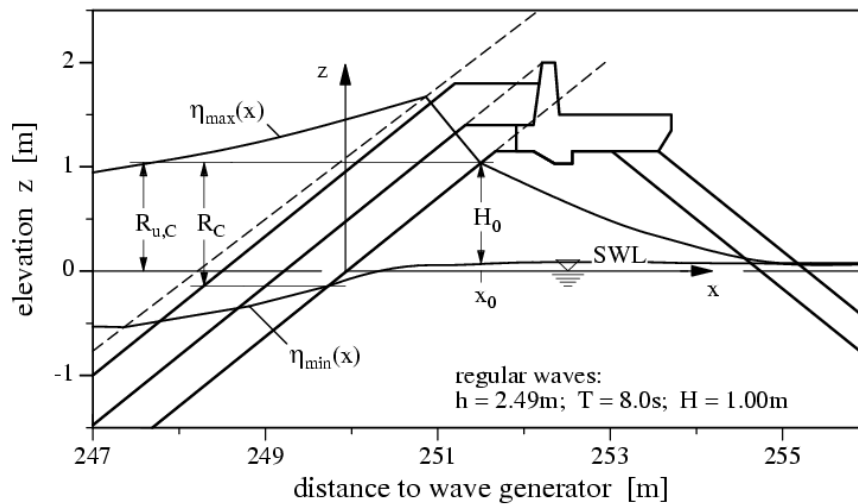


Figure 1: Definition sketch for the analysis of wave damping inside the breakwater core

The wave height at the point of maximum wave run-up between the core and the filter layer is considered as the initial wave height  $H_0$ . The core material is assumed to be homogeneous. It is further assumed that the wave damping inside the core at  $x \geq x_0$  is not directly affected by the wave

transformation at the seaward slope (except for the initial wave height  $H_0$ ). Thus, wave damping inside the breakwater core and the infiltration process at the slope are considered as two separate and successive processes.

### THEORETICAL WAVE DAMPING APPROACH

The relationship between hydraulic gradient  $I$  and discharge velocity  $v_f$  is determined by the extended Forchheimer equation (equation 1). The wave damping inside a rubble mound breakwater, which is closely linked to the hydraulic resistance, can be approximated by the following approaches that have been derived from the extended Forchheimer equation.

The discharge velocity  $v_f(x, z, t)$  is replaced by a depth averaged ( $z = 0 \rightarrow -h$ ) and time averaged ( $t = 0 \rightarrow T$ ) velocity  $v_m(x)$ , which is approximated by (see also MUTTRAY, 2000):

$$v_m = \kappa_v H(x)$$

$$\kappa_v = \frac{n}{\pi} \frac{\omega}{k' h} \left[ 1 + \frac{2}{\pi} \left( 1 - \frac{\cosh(k' h)}{\cosh(1.5 k' h)} \right) \right] \quad \text{Eq. 7}$$

with local wave height  $H(x)$ , circular frequency  $\omega = 2 \pi/T$ , internal wave number  $k' = 2 \pi/k'$  (internal wave length  $L'$ ), water depth  $h$ , porosity  $n$  and velocity coefficient  $\kappa_v$  [1/s].

An average hydraulic gradient  $I_m(x)$  (averaged over water depth and wave period) corresponds to the average pressure gradient for constant water depth. The gradient  $I_m(x)$  can be approximated by the gradient of the average height of the pressure oscillations  $P_m(x)/\delta x$  or by the gradient of the wave height  $H_m(x)/\delta x$  if the water surface and pressure oscillations are approximately sinusoidal and if their variation over the water depth is negligible (MUTTRAY, 2000). The hydraulic resistance  $I_m(x) = f(v_m)$  with  $v_m$  according to equation 7, is thus described by:

$$I_m(x) = -\text{grad} \left( \frac{p(x)}{\rho g} \right) \approx -\frac{2}{\pi} \frac{\delta P_m(x)}{\delta x} \approx -\frac{2}{\pi} \frac{\delta H(x)}{\delta x} = f(\kappa_v H(x)) \quad \text{Eq. 8}$$

which might result in a linear, quadratic or polynomial damping function.

Damping functions for laminar flow (linear damping), fully turbulent flow (quadratic damping) and combined laminar and turbulent flow are derived in Table 3. The damping coefficients for linear and quadratic damping correspond to the Forchheimer coefficients  $a$  and  $b$ , respectively. A linear damping results in an exponential decrease of wave height. If turbulent and laminar flow both occur in different sections of the porous medium the hydraulic gradient is approximated by the sum of linear and quadratic resistance terms.

A variation of the initial wave height  $H_0$  is associated with a corresponding variation of the local damped wave height  $H(x)$  only in the case of linear damping. In the case of quadratic damping a significant variation of the initial wave height  $H_0$  will after a certain distance cause only a very limited variation of the local wave heights  $H(x)$ . A similar trend can be seen for the polynomial damping which of course depends on the relative importance of the quadratic resistance.

Boundary condition	$H(x=0) = H_0$	
<b>Linear damping approach</b>	Laminar flow	
Basic equation:	$-\frac{2}{\pi} \frac{\delta H(x)}{\delta x} = a \kappa_v H(x)$	
Local wave height:	$H(x) = H_0 \exp\left[-\frac{\pi}{2} a \kappa_v x\right]$	Eq. 9
<b>Quadratic damping approach</b>	Fully turbulent flow	
Basic equation:	$-\frac{2}{\pi} \frac{\delta H(x)}{\delta x} = b(\kappa_v H(x))^2$	
Local wave height:	$H(x) = \frac{H_0}{\frac{\pi}{2} b \kappa_v^2 H_0 x + 1}$	Eq. 10
<b>Polynomial damping approach</b>	Laminar and turbulent flow	
Basic equation:	$-\frac{2}{\pi} \frac{\delta H(x)}{\delta x} = a \kappa_v H(x) - b(\kappa_v H(x))^2$	
Local wave height:	$H(x) = \frac{a}{\exp\left[\frac{\pi}{2} a \kappa_v x\right] \left(\frac{a}{H_0} + b \kappa_v\right) - b \kappa_v}$	Eq. 11

Table 3: Linear, quadratic and polynomial damping functions

### EXPERIMENTAL INVESTIGATIONS

The experimental set-up in the Large Wave Flume (GWK) in Hanover consists of a 1:50 foreshore of 100 m length and a rubble mound breakwater with typical cross section. The breakwater has 1:1.5 slopes. The seaward slope is protected by an Accropode armour layer with a unit weight of 40 kg. The underlayer consists of crushed rock (rock size 80/150 mm with an average weight of 1.95 kg. The breakwater core has a crest width of 1.35 m and a crest height of 3.75 m (Figure 2). The core material consists of gravel (rock size 22/56 mm); the geometric properties of the core material, the resistance coefficients of the extended Forchheimer equation for an oscillating single phase flow and their contribution to the total flow resistance are summarised in Table 4 (for further details see van Gent, 1993 and Muttray, 2000).

	Equivalent diameter	Nominal diameter		
Rock size	$d_{eq} = 0.0385$ m	$d_{n15} = 0.023$ m	$d_{n50} = 0.031$ m	$d_{n85} = 0.040$ m
Non-uniformity	1.51			
Porosity	0.388			
Hydraulic resistance		Laminar	Turbulent	Inertia
Forcheimer coefficient		$a = 0.89$ s/m	$b = 22.9$ s <sup>2</sup> /m <sup>2</sup>	$c = 0.26$ s <sup>2</sup> /m
Contribution to total resistance		11%	83 – 87%	2 – 6%

Table 4: Geometric properties of the core material, resistance coefficients and their contribution to the total flow resistance for oscillatory flow

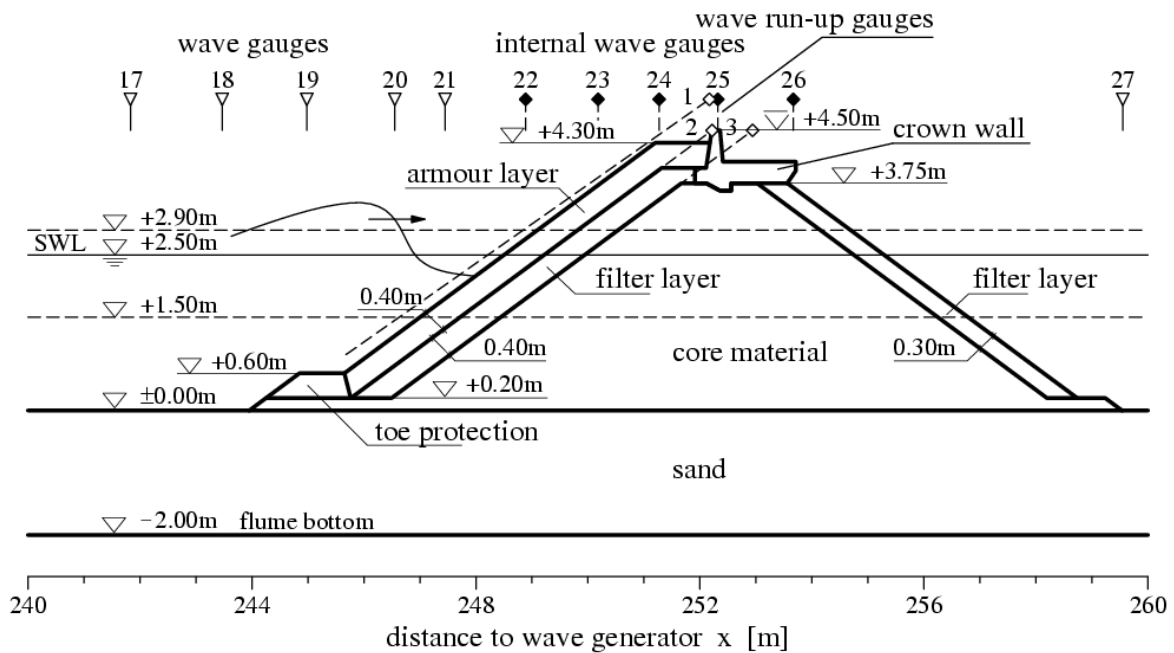


Figure 2: Cross section of the breakwater model with wave gauges and wave run-up gauges

The wave motion inside the structure has been determined from the water surface elevations inside the core (wave gauges 22 – 26) and at the seaward slope on the armour layer, on the filter layer and on the breakwater core (wave run-up gauges 1 – 3). Modified wave gauges, which are protected by a cage against the surrounding rock material, have been applied for wave height and for wave run-up measurements inside the structure. The position of wave gauges and wave run-up gauges can be seen in Figure 2. Details of the data collection, processing and analysis can be found in Muttray (2000).

A typical breakwater configuration has been tested in the GWK; the structural parameters (geometry and rock material) have not been varied with respect to the large model scale. The wave parameters and the water level have been varied systematically (see Table 5). The relative water depth  $h/L$  varies from 0.05 to 0.23 ( $kh = 0.35$  to 1.45) and is thus transitional and close to shallow water conditions. The wave steepness  $H/L$  varies from 0.005 to 0.056 and the relative wave height  $H/h$  varies between 0.09 and 0.4. The range of surf similarity parameters  $\xi = \tan[\alpha/(H/L_0)^{1/2}]$  is 3.0 to 16.7.

Two water levels ( $h = 2.50$  m and 2.90 m) have been considered. Wave overtopping was practically excluded from these tests in order to avoid any infiltration into the breakwater core from the breakwater crest. Therefore the maximum wave heights at water level  $h = 2.50$  m and 2.90 m were limited to  $H = 1.0$  m and 0.7 m, respectively.

Tests have been conducted with regular waves and wave spectra. Regular wave tests give insight into the hydraulic processes and have been used for the validation of theoretical approaches as well as for empirical adjustments and extensions. Wave spectra have been tested to check the applicability of regular wave results for irregular waves.

Water level [m]	Wave period $T, T_p$ [s]	Regular waves Wave height $H_s$ [m]	Wave spectra Wave height $H_{m0}$ [m]
2.5	4, 5, 6, 8, 10	0.25 – 1.00	0.25 – 1.00
2.9	3, 4, 5, 6, 8, 10	0.25 – 0.70	0.25 – 0.70

Table 5: Test programme

### EXPERIMENTAL RESULTS

The decrease of wave height inside the breakwater core is plotted in Figure 3 against the distance  $x - x_0$  (see Figure 1) for regular waves (wave period  $T = 4$  s, 8 s, wave height  $H = 0.25$  m, 0.40 m, 0.55 m, 0.70 m and water level  $h = 2.50$  m). The initial wave height  $H_0$  at position  $x_0$  varies significantly with the incident wave height (constant wave period). For shorter waves ( $T = 4$  s) the wave height inside the breakwater core approaches after a relatively short distance a value that is almost independent of the initial wave height. Once this value is reached, the wave damping decreases significantly. A similar effect can be seen for longer waves ( $T = 8$  s). A quadratic or polynomial damping approach appears to be more suitable for the wave height decay inside a breakwater than a linear damping approach.

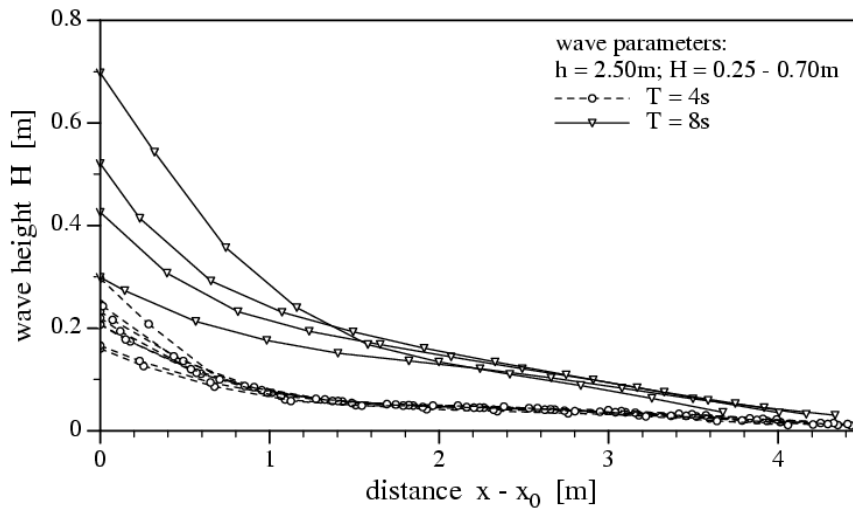


Figure 3: Variation of wave height inside the breakwater core with distance  $x - x_0$  for various incident wave heights and wave periods

The applicability of the damping functions (equations 9, 10 and 11, Table 3) for the wave height attenuation inside the breakwater is addressed below. The velocity coefficient  $\kappa_v$  according to equation 7 is about  $0.25 \text{ s}^{-1}$  (with a standard deviation of  $0.011 \text{ s}^{-1} = 4.5\%$ ) for the wave conditions that have been tested.

**Linear damping:** The coefficient  $a$  of the linear damping function (equation 9) is considered as a linearised resistance coefficient  $a_{eq}$  and is therefore different from the linear hydraulic resistance coefficient  $a$  of the Forchheimer equation. The linearised resistance coefficient  $a_{eq}$  can be approximately determined according to MUTTRAY (2000):

$$a_{eq} = a + \frac{1}{36} H \frac{gb}{\sqrt{ch}} \left[ 1 + \frac{k'h}{4} - \frac{2}{5} \tanh(k'h) \right] \quad \text{Eq. 12}$$

For this experimental investigations the coefficient  $a_{eq}$  is about 2 in average (with coefficients  $a$ ,  $b$  and  $c$  according to Table 1). The wave number  $k'$  inside the structure has been determined according to the linearised dispersion equation (see MUTTRAY, 2000):

$$\omega^2 = \frac{k'}{nc} \tanh(k'h) \quad \text{Eq. 13}$$

An average wave height of  $H = 0.43 H_0$  has been considered. This wave height corresponds to the average height of waves with exponentially decreasing height that travel 3 m inside the structure (according to 9) if the wave height at the landward end of the core is neglected.

The applicability of the linear damping approach (equation 9) for the wave decay inside the breakwater core is demonstrated in Figure 4.

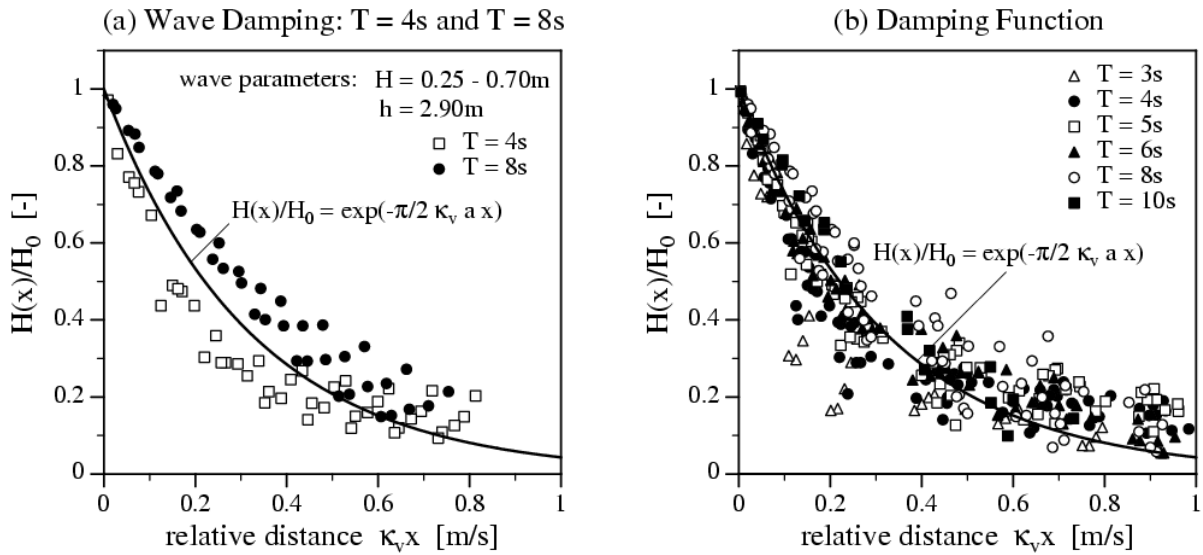


Figure 4: Linear wave damping approach: (a) wave decay for longer ( $T = 8$  s) and shorter ( $T = 4$  s) wave periods, (b) wave decay vs. relative distance  $\kappa_v x$

The differences between measured and calculated wave height decay (according to equation 9) are shown exemplarily for a number of tests with shorter and longer wave periods in Figure 4a (with  $a = 2$  s/m and  $\kappa_v \approx 0.25$  s<sup>-1</sup>). The damping rate of longer wave periods ( $T = 8$  s) is overestimated in the seaward part of the breakwater core while the damping rate of shorter wave periods ( $T = 4$  s) is underestimated.

The wave height evolution inside the core is plotted in Figure 4b against the relative distance  $\kappa_v x$  for all tests. It is obvious that the wave heights in the landward part of the breakwater core ( $\kappa_v x > 0.6$ ) are underestimated by this approach. The measured wave heights are in average 2.5% smaller than the calculated wave heights; the standard deviation is 0.028 m (18.2%).

Even with the systematic deviations between calculated and measured wave heights it can be concluded that the linear damping approach (equation 9) provides a very simple and relatively accurate approximation for the wave damping inside the breakwater core.

**Quadratic damping:** The applicability of the quadratic damping approach according to equation 10 is shown in Figure 5. If the experimentally determined quadratic Forchheimer coefficient  $b = 22.9 \text{ s}^2/\text{m}^2$  is applied as a damping coefficient the wave height inside the structure is underestimated in average by 16.3% with a standard deviation between measured and predicted wave heights of 0.052 m (33.9%). As the quadratic damping coefficient  $b$  varies with the relative water depth  $\omega^2 h/g$  it has been empirically approximated by  $b = (3 + 26 \omega^2 h / g) / (g d_{n50})$ .

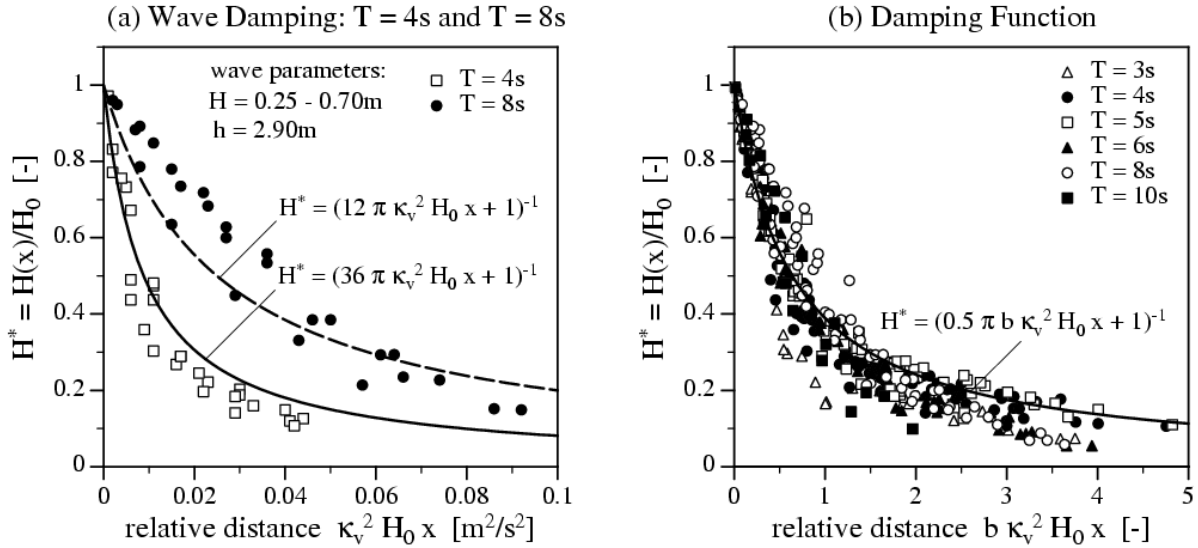


Figure 5: Quadratic wave damping approach: (a) wave decay for longer ( $T = 8 \text{ s}$ ) and shorter ( $T = 4 \text{ s}$ ) wave periods, (b) wave decay vs. relative distance  $b \kappa_v^2 H_0 x$ .

The differences between measured and calculated wave height decay (according to equation 10) are shown exemplarily for a number of tests with shorter and longer wave periods in Figure 5a. The wave decay is plotted against  $b \kappa_v^2 H_0 x$ . The damping coefficient  $b$  varies with  $\omega^2 h/g$  and thus the wave damping is different for long and short period waves. Generally, the quadratic damping function appears to be slightly closer to the actual wave damping than the linear approach (see Figure 4a).

The wave damping inside the breakwater is plotted in Figure 5b against the relative distance  $b \kappa_v^2 H_0 x$  for all tests. The wave heights in the seaward part of the structure are slightly underestimated while the wave heights in the landward part are slightly overestimated. The systematic deviation between measured and calculated wave heights is only 0.1%, the standard deviation is 0.032 m (21.1%).

The wave decay inside the breakwater is qualitatively better reproduced by the quadratic damping function than by the linear damping model. However, the effect of wave length is not properly described by the velocity coefficient. This shortcoming will affect the results from the quadratic approach more than the results of the linear approach ( $\kappa_v$  is linear in equation 9 and quadratic in equation 10). Hence the scatter between measured and predicted wave heights inside the structure is larger for the quadratic approach than for the linear approach even though the physics of the wave damping process inside a breakwater are better described by the quadratic approach. The over-simplified velocity coefficient  $\kappa_v$  can be partly compensated by an empirical correction of the resistance coefficient  $b$  as a function of  $\omega^2 h/g$ . For the present case the relative standard deviation can be reduced from 33.9% to 21.1%. However, the general applicability of such a purely empirical correction is uncertain.

**Polynomial damping:** The applicability of the polynomial damping approach according to equation 11 is shown in Figure 6. If the experimentally determined linear and quadratic Forchheimer coefficients  $a = 0.89$  s/m and  $b = 22.9$  s<sup>2</sup>/m<sup>2</sup> are applied the wave heights inside the breakwater are underestimated in average by 8.0% with a standard deviation of 0.046 m (32.7%). In order to compensate the effect of wave length that is not sufficiently taken into account by the coefficient  $\kappa_v$  the quadratic damping coefficient  $b$  has been empirically approximated by  $b = 9k'h/(gd_{n50})$ .

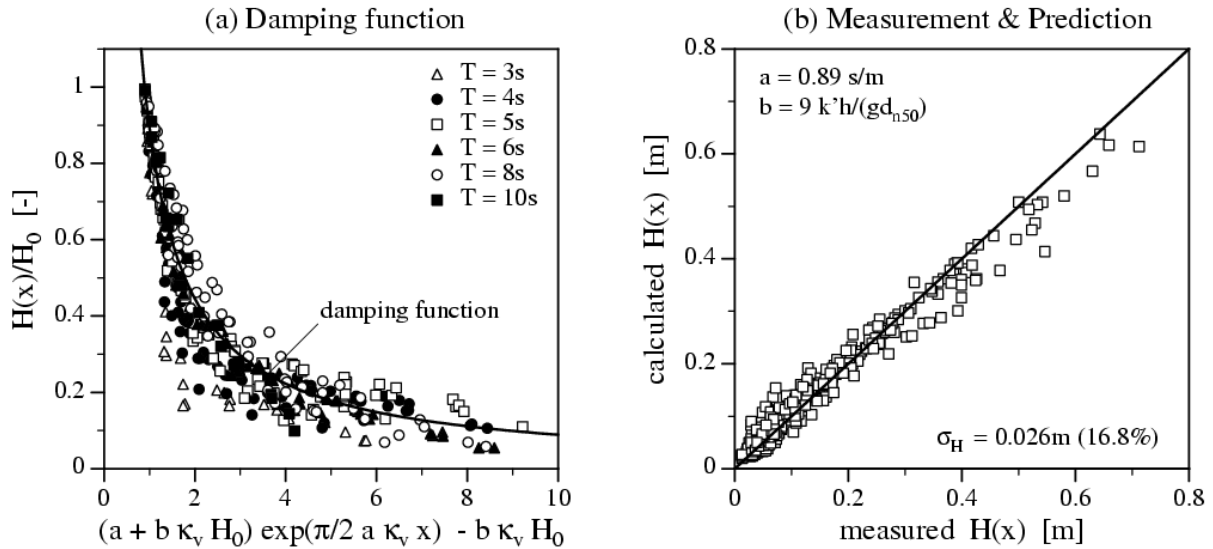


Figure 6: Polynomial wave damping approach: (a) wave decay inside the breakwater core, (b) comparison of measured and calculated local wave heights  $H(x)$

The wave decay inside the breakwater core (according to equation 11) is plotted in Figure 6a against the relative distance  $(a + b \kappa_v H_0) \exp(0.5 \pi a \kappa_v x) - b \kappa_v H_0$ . The wave heights in the most seaward part of the structure are slightly underestimated by the polynomial approach while the wave heights further landwards are approximated very well. The calculated wave heights are in average 2.2% larger than the measured values and have a the standard deviation of 0.026m (16.8%) (Figure 6b). It can be concluded that the polynomial approach according to equation 11 (with an empirical adaptation of the quadratic resistance coefficient  $b$ ) provides a good approximation of the actual wave height decay inside a breakwater. As for the quadratic approach (equation 10) the accuracy of the results is limited due to the fact that the coefficient  $\kappa_v$  that does not cover the effect of wave length completely.

**Extended polynomial approach:** In order to consider the effect of wave length on the wave damping properly an empirical coefficient  $\kappa_x$  is added to the polynomial damping approach (equation 11):

$$H(x) = \frac{a}{\exp\left[\frac{\pi}{2} a \kappa_v \kappa_x x\right] \left(\frac{a}{H_0} + b \kappa_v\right) - b \kappa_v} \quad \text{Eq. 14}$$

For regular and irregular waves the wave decay inside the breakwater core according to equation 14 is plotted in Figure 7a and b. The experimentally derived Forchheimer coefficients  $a = 0.89$  s/m and

$b = 22.9 \text{ s}^2/\text{m}^2$  (see Table 4) and an internal wave number  $k'$  that has been derived from the linearised dispersion equations (in the present case:  $k' \approx k$ , for details MUTTRAY, 2000) have been applied. The following empirical coefficients  $\kappa_x$  have been used:

$$\begin{aligned} \text{regular waves} \quad \kappa_x &= 1.5 k' h \\ \text{wave spectrum} \quad \kappa_x &= 1.25 k' h \end{aligned} \tag{Eq. 15}$$

For *regular waves* the local wave heights inside the structure according to equation 14 are in average 0.6% larger than the measured wave heights, the standard deviation is 0.021 m (14.9%) (Figure 7). It can be seen that the actual wave height decay inside a breakwater core is well described by the extended polynomial approach (equation 14).

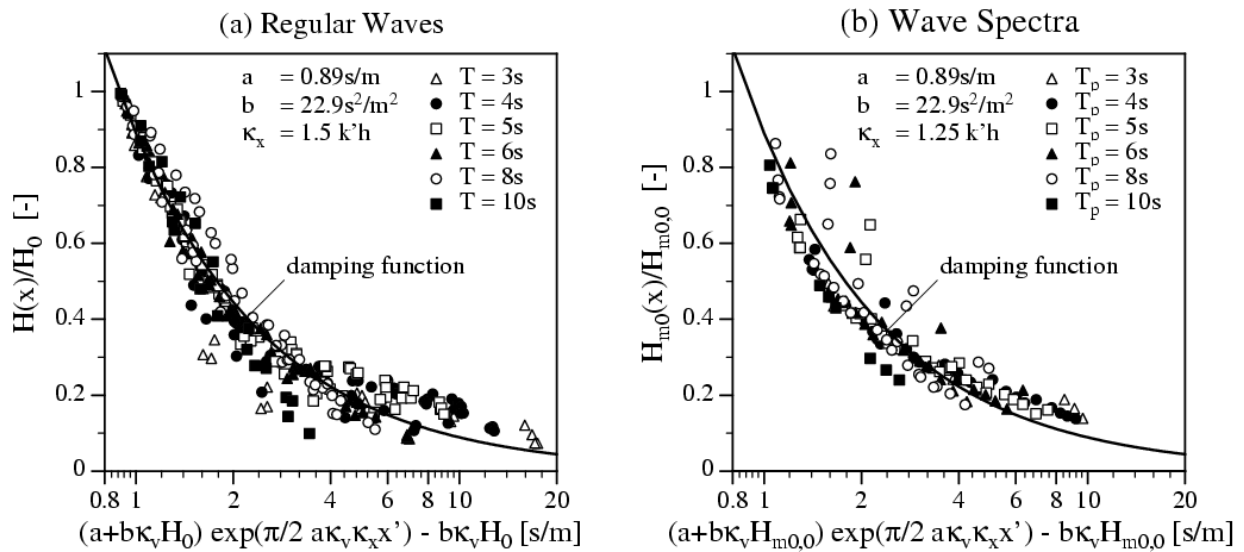


Figure 7: Extended polynomial wave damping approach: (a) regular waves, (b) wave spectra

For *wave spectra* the calculated wave heights inside the structure are in average 2.6% smaller than the measured wave heights, the standard deviation is 0.039 m (29.5%) (Figure 7b). The wave heights in the seaward part of the breakwater core are slightly overestimated while the wave heights further landwards are slightly underestimated. In some of the experiments with wave periods  $T_p = 5 \text{ s}$ ,  $6 \text{ s}$  and  $8 \text{ s}$  the wave height measurements are distorted by "internal wave overtopping" (the wave run-up at the intersection between filter layer and core reaches the crest the breakwater and generates an additional water surface for the wave gauges in this part of the breakwater). It appears as if these waves were propagating a certain distance into the breakwater without significant damping. In all cases without "internal wave overtopping" the decay of significant wave heights  $H_{m0}$  inside the breakwater can be reasonably assessed by equation 14 for irregular waves.

## CONCLUDING REMARKS

A theoretical approach for the wave damping inside a rubble mound breakwater has been derived for a homogeneous core material. The wave kinematics are described by linear wave theory, the discharge velocity has been averaged (over wave period and water depth). The hydraulic gradient is approximated by the wave height gradient. The wave length inside the structure has been determined from a linearised dispersion equation for porous media, the effect of instationary flow has not been considered explicitly. The outcome is a linear model (for laminar flow), a quadratic model (for turbulent flow) and a polynomial model (for combined laminar and turbulent flow) for the wave height decay inside the breakwater. Despite these assumptions and simplifications the

damping functions that have been derived reflect the governing physical processes better than available approaches such as equation 6.

The wave damping inside the breakwater can be reasonably approximated by a linear damping model and the corresponding exponential decrease. However, the choice of the damping coefficient is a relatively difficult task. The Forchheimer coefficient  $a$  is not appropriate and has to be replaced by an equivalent linear damping coefficient  $a_{eq}$ , which takes both laminar and turbulent losses into account and depends on the flow field inside the breakwater.

A quadratic damping model with Forchheimer coefficient  $b$  as damping coefficient does not provide a significant improvement while a polynomial approach appears to be very promising. The latter is mainly advantageous due to the fact that Forchheimer coefficients  $a$  and  $b$  can be directly applied as damping coefficients in the polynomial model. As the polynomial damping model slightly underestimates the effect of wave length an empirical correction has been introduced.

The extended polynomial damping model has been validated against results from regular and irregular wave tests. The new approach is applicable for porous media for which the hydraulic resistance can be approximated by the Forchheimer equation. The formulae are not restricted to a certain breakwater geometry or wave conditions. However, in the case of wave overtopping or "internal wave overtopping" (infiltration into the core from the breakwater crest) the pressure distribution inside the breakwater and the internal wave decay may differ significantly from the proposed models.

The main tasks for future research are:

- A more rational physically based justification for the empirical correction factor  $\kappa_x$ , which is very important to conclude on the general applicability the polynomial damping model;
- Analysis of the internal flow field including air entrainments in case of wave overtopping;
- Analysis of the hydraulic processes in the seaward part of the breakwater core that is directly affected by the wave transformation on the slope;

## ACKNOWLEDGEMENTS

The support of the German Research Foundation (DFG) [Basic Research Unit SFB 205, project B13 ("Design of rubble mound breakwaters") and research programme "Design wave parameters for coastal structures" (Ou 1/3-1,2,3)] and of Delta Marine Consultants b.v. is gratefully acknowledged. Further the essential contributions of Christian Pabst amongst many others in the experimental study, of Erik Winkel in the data analysis and of Dr. Deborah Wood in the theoretical study shall be mentioned.

## REFERENCES

- BUERGER, W.; OUMERACI, H.; PARTENSKY, H.W. (1988): Geohydraulic investigations of rubble mound breakwaters. ASCE; *Proceedings ICCE*; Vol. 21, pp. 15.
- CARMAN, P.C. (1937): Fluid flow through granular beds. *Trans. Inst. of Chemical Eng.*; Vol. 15, pp. 150-166.
- ENGELUND, F.A. (1953): On the laminar and turbulent flow of groundwater through homogeneous sand. *Transactions Danish Academy of Technical Sciences*; Vol. 3, No. 4, pp. 1.
- ERGUN, S.; ORNING, A.A. (1949): Fluid flow through randomly packed columns and fluidized beds. *Journal of Industrial Eng. Chemistry*; Vol. 41, No. 6, pp. 1179-1189.
- ERGUN, S. (1952): Fluid flow through packed columns. *Chem. Engrg. Progress*; Vol. 48, pp. 89-94.

- GENT, M.R.A. VAN (1993): Stationary and oscillatory flow through coarse porous media. Faculty of Civil Engineering; *Communications on Hydraulic and Geotechnical Engineering*; Report No. 93-9; pp. 61; Delft University of Technology.
- HALL, K.R. (1991): Trends in phreatic surface motion in rubble-mound breakwaters. ASCE; *Journal of Waterway, Port, Coastal, and Ocean Engineering*; Vol. 117, No. 2, pp. 179-187.
- HALL, K.R. (1994): Hydrodynamic pressure changes in rubble mound breakwater armour layers. IAHR; *Proceedings International Symposium: Waves - Physical and Numerical Modelling*; pp. 1394-1403.
- KOENDERS, M.A. (1985): Hydraulic criteria for filters. Delft Geotechnics, unnumbered Report; Estuary Filters.
- KOZENY, J. (1927): Ueber kapillare Leitung des Wassers im Boden. *Sitzungs-Berichte der Wiener Akademie der Wissenschaft*; Rep. 11a; pp. 271-306.
- MUTTRAY, M.; OUMERACI, H.; ZIMMERMANN, C.; PARTENSKY, H.-W. (1992): Wave energy dissipation on and in rubble mound breakwaters. ASCE; *Proceedings ICCE*; Vol. 23, pp. 1434-1447.
- MUTTRAY, M.; OUMERACI, H.; ZIMMERMANN, C. (1995): Wave-induced flow in a rubble mound breakwater. *Proceedings COPEDEC*; Vol. 4, pp. 1219-1231.
- MUTTRAY, M. (2000): Wellenbewegung an und in einem geschuetteten Wellenbrecher – Laborexperimente im Grossmassstab und theoretische Untersuchungen. *Ph.D. Thesis*; Techn. University Braunschweig; Dept. of Civil Engineering; pp. 282.
- OUMERACI, H.; PARTENSKY, H.W. (1990): Wave-induced pore pressure in rubble mound breakwater. ASCE; *Proceedings ICCE*; Vol. 22, pp. 14.
- POLUBARINOVA-KOCHINA, P.Y. (1962): Theory of groundwater movement. Princeton University Press; Princeton, N.J.
- SHIH, R.W.K. (1990): Permeability characteristics of rubble material - new formulae. ASCE; *Proceedings ICCE*; Vol. 22, No. 2, pp. 1499-1512.
- SOLLIT, C.K.; CROSS, R.H. (1972): Wave transmission through permeable breakwaters. ASCE; *Proceedings ICCE*; Vol. 13, pp. 1827-1846.
- TROCH, P.; DE SOMER, M.; DE ROUCK, J.; VAN DAMME, L.; VERMEIR, D.; MARTENS, J.P., VAN HOVE, C. (1996): Full scale measurements of wave attenuation inside a rubble mound breakwater. ASCE; *Proceedings ICCE*; Vol. 25, No. 2, pp. 1916-1929.
- TROCH, P.; DE ROUCK, J.; VAN DAMME, L. (1998): Instrumentation and prototype measurements at the Zeebrugge rubble mound breakwater. *Coastal Engineering*; Vol. 35, No. 1/2, pp. 141-166.